arXiv:1903.04742v1 [astro-ph.CO] 12 Mar 2019

Astro2020 Science White Paper

Testing the Nature of Dark Matter with Extremely Large Telescopes

Thematic Areas: ☐ Planetary Systems ☐ Star and Planet Formation
☐ Formation and Evolution of Compact Objects ☑ Cosmology and Fundamental Physics
☐ Stars and Stellar Evolution ☐ Resolved Stellar Populations and their Environments
☐ Galaxy Evolution ☐ Multi-Messenger Astronomy and Astrophysics

Principal Author:
Name: Joshua D. Simon
Institution: Carnegie Observatories
Email: jsimon@carnegiescience.edu

Co-authors: Simon Birrer (UCLA), Keith Bechtol (University of Wisconsin-Madison), Sukanya Chakrabarti (RIT), Francis-Yan Cyr-Racine (Harvard University & University of New Mexico), Ian Dell'Antonio (Brown), Alex Drlica-Wagner (Fermilab), Chris Fassnacht (UC Davis), Marla Geha (Yale), Daniel Gilman (UCLA), Yashar D. Hezaveh (Flatiron Institute), Dongwon Kim (UC Berkeley), Ting S. Li (Fermilab), Louis Strigari (Texas A&M), and Tommaso Treu (UCLA)

Abstract: For nearly 40 years, dark matter has been widely assumed to be cold and collisionless. Cold dark matter models make fundamental predictions for the behavior of dark matter on small ($\lesssim$ 10 kpc) scales. These predictions include cuspy ($\rho \propto r^{-1}$) density profiles at the centers of dark matter halos and a halo mass function that increases as $dN/dM \propto M^{-1.9}$ down to very small masses. We suggest two observational programs relying on extremely large telescopes to critically test these predictions, and thus shed new light on the nature of dark matter. (1) Combining adaptive optics-enabled imaging with deep spectroscopy to measure the three-dimensional motions of stars within a sample of Local Group dwarf galaxies that are the cleanest dark matter laboratories known in the nearby universe. From these observations the inner slope of the dark matter density profile can be determined with an accuracy of 0.20 dex, enabling a central cusp to be distinguished from a core at 5σ significance. (2) Diffraction-limited AO imaging and integral field spectroscopy of gravitationally lensed galaxies and quasars to quantify the abundance of dark substructures in the halos of the lens galaxies and along the line of sight. Observations of 50 lensed arcs and 50 multiply-imaged quasars will be sufficient to measure the halo mass function over the range $10^7 < M < 10^{10}$ $M_\odot$ at cosmological scales, independent of the baryonic and stellar composition of those structures. These two observational probes provide complementary information about the small scale structure, with a joint self-consistent analysis mitigating limitations of either probe. This program will produce the strongest existing constraints on the properties of dark matter on small scales, allowing conclusive tests of alternative warm, fuzzy, and self-interacting dark matter models.

1 The Astrophysics of Dark Matter

The nature of dark matter remains one of the most important questions in physics. Because of the tremendous overall successes of the dark energy + cold dark matter (ΛCDM) model, dark matter is widely assumed to consist of a massive, weakly-interacting particle. However, decades of effort to detect such a particle with accelerators, direct detection experiments, and indirect searches for the products of dark matter annihilation or decay have thus far failed to identify any signature of the dark matter particle. At present, astrophysical measurements still represent our only means of directly studying the properties of dark matter.

1.1 Problems on Small Scales

Although the large-scale structure of the universe is in excellent agreement with the predictions of the ΛCDM paradigm, numerical simulations have identified possible discrepancies with the observed properties of galaxies on small scales (< 10 kpc). In particular, in the absence of self-interactions or interactions with baryons, halos composed of massive dark matter particles should follow a universal density profile, with $\rho \propto r^{-1}$ at small radii and $\rho \propto r^{-3}$ at large radii (e.g., Navarro et al., 1996, 2004). However, observations of dark matter-dominated galaxies and galaxy clusters generally find shallower density profiles, in some cases with nearly constant-density central cores (e.g., Oh et al., 2011, 2015; Newman et al., 2013; Adams et al., 2014). This cusp-core problem has persisted for 25 years despite major improvements in both simulations and observations. Currently-favored explanations for the problem include modifications to the gravitational potential of galaxies by repeated episodes of strong stellar feedback (e.g., Governato et al., 2012) or self-interacting dark matter models (e.g., Spergel & Steinhardt, 2000; Kaplinghat et al., 2016). Simulations also predict that the dark matter halo mass function rises steeply ($dN/dM \propto M^{-1.9}$; Springel et al. 2008) with decreasing mass down to the free-streaming scale ($\sim 10^{-6}$ M$_\odot$ for GeV-mass dark matter particles). On the other hand, the galaxy luminosity function has a significantly shallower slope, and if all low-mass dark matter halos above $\sim 10^8$ M$_\odot$ contain galaxies then the Milky Way hosts many fewer satellite galaxies than expected (Klypin et al., 1999; Moore et al., 1999). While this missing satellite problem can be explained by restricting galaxy formation to specific subsets of the dark matter halo population (e.g., Kravtsov 2010), the existence of halos with masses smaller than those of galaxies is a fundamental — and testable — prediction of CDM (e.g., Bullock & Boylan-Kolchin 2017). Thus, although there are plausible explanations for these problems without invoking a crisis for the ΛCDM model, new observations are required to verify the proposed solutions and demonstrate that the predictions of ΛCDM on small scales are accurate.

1.2 Testing ΛCDM

Local volume: Measurements of dark matter density profiles in the nearby universe have generally focused on low-mass disk galaxies, which contain significant baryonic components. Episodes of star formation in these systems may substantially alter the original distribution of dark matter (e.g., Di Cintio et al., 2014), making the measurements difficult to interpret in the context of the prediction of central cusps. Ideally, one would prefer to determine the density profiles of the most dark matter-dominated objects known, namely the dwarf galaxies orbiting the Milky Way. The smallest of these galaxies are so dark matter-dominated that stellar feedback is unlikely to have affected their dark matter halos on ~ 100 pc scales (e.g., Bullock & Boylan-Kolchin 2017). Many studies have attempted to constrain the dark matter distribution in Milky Way dwarf spheroidals via line-of-sight velocity measurements, but the degeneracy between the mass profile and the orbital

anisotropy of the stars has led to conflicting results (e.g., Battaglia et al., 2008; Amorisco & Evans, 2012; Breddels et al., 2013; Strigari et al., 2017).

Similarly, a number of methods have been used to attempt to detect the dark (or nearly dark) subhalos predicted by ΛCDM in the Local Group and surrounding regions. These techniques include searches for galaxies associated with low-mass gas clouds (e.g., Simon & Blitz, 2002; Adams et al., 2016), searches for gaps in tidal streams (e.g., Carlberg, 2012; Bonaca et al., 2018), and analyses of their visible gravitational signatures on the outer gas disks of galaxies (Chakrabarti & Blitz, 2009; Chakrabarti et al., 2011). While each of these approaches continues to hold promise, it is not clear at present whether any of them will yield definitive results.

Cosmological distances: Strong gravitational lensing offers a unique way to detect low-mass dark matter halos at cosmological distances (e.g., Mao & Schneider, 1998; Metcalf & Madau, 2001; Dalal & Kochanek, 2002; Koopmans, 2005). Because gravitational lensing is affected only by the projected mass surface density, it is sensitive to mass concentrations independent of their baryonic content. Thus, purely dark halos can be detected, providing a stringent test of dark matter models. Identified structures include both subhalos within the primary lensing galaxy ("substructure") and halos along the line of sight between the lensed object and the observer ("LOS structure"; Li et al. 2017; Despali et al. 2018).

Lensing substructure can alter both the distortion of extended lensing arcs and the magnification of unresolved sources. Induced distortions in extended Einstein rings, a method known as gravitational imaging, have resulted in the detection of substructure with inferred lensing masses of $M_{\rm lens} \approx 10^{8-9}$ $M_\odot$ with HST, Keck AO and ALMA data (Vegetti et al., 2010, 2012, 2014; Hezaveh et al., 2016; Birrer et al., 2017; Ritondale et al., 2019). The sensitivity limit of a lensing detection is set by the angular resolution of the data and the structure of the lensed source. Additional modeling challenges arise as a result of the complexity of the data set, uncertainties in telescope and instrument response and degeneracies in the lens model and source structure.

Unresolved magnification effects have been probed by examining the flux ratios between neighboring images of multiply-imaged quasars. These data are consistent with CDM at scales of $\gtrsim 10^9$ $M_\odot$ (Dalal & Kochanek, 2002; Nierenberg et al., 2017). However, existing observations lack sufficient resolution to probe interesting regimes of viable warm dark matter models, which require reaching $\sim 10^7$ $M_\odot$. The magnification ratio and thus the interpretation of the flux ratios depends on the size of the emitting source region (radio vs. narrow-line emission region) and on the smooth component of the lens model with respect to which anomalies can be identified. Oversimplified lens models can bias the expected flux ratios (Xu et al., 2016), and baryonic structures can affect the interpretation of anomalous structures in both real lenses (Hsueh et al., 2016, 2017, 2018) and simulated ones (Gilman et al., 2017). Exploiting the full power of lensing to constrain the nature of dark matter will require both sophisticated analysis tools **and** exquisite data, which can only be obtained with the angular resolution and collecting area of extremely large telescopes (ELTs).

2 An Observational Path Forward

Dwarf galaxy kinematics: Combined radial velocity and proper motion measurements for stars in a dwarf galaxy would tightly constrain the stellar orbits within the galaxy and break the degeneracies that have plagued previous density profile studies. Obtaining such 3D motions requires both spectroscopy and high-precision astrometry. Theoretical modeling suggests that velocity measure-

ments accurate to $\sim$ 3 km s^{-1} in each dimension for a sample of $\sim$ 300 stars is the minimum necessary to reliably recover the gravitational potential (e.g., Strigari et al., 2007). Proper motions of faint dwarf galaxy stars at the required accuracy can only be measured with laser guide star AO imaging. Here the AO field of view is critical, because the surface density of member stars at the relevant magnitudes is < 0.1 arcsec^{-2}, requiring large fields to obtain the sample needed to determine the tangential velocity dispersion. A velocity uncertainty of 3 km s^{-1} translates to a proper motion uncertainty of $6.3\ (100\ \mathrm{kpc}/d)\ \mu$as yr^{-1}, or 7.9 (21.0) μas yr^{-1} at a distance of 80 (30) kpc. With the anticipated $\sim$ 15 μas astrometric error floor of a 30 m telescope (Wright et al., 2016), these proper motions could be measured over a time baseline of a few years.

Radial velocities for dwarf galaxy member stars can be obtained with multi-object spectrographs on large (> 6 m) telescopes. Velocity measurements for faint stars have been demonstrated at the 1.5 km s^{-1} level at $R = 6000$ (Keck/DEIMOS; Kirby et al., 2015) and the 1.0 km s^{-1} level at $R = 12000$ (Magellan/IMACS; Simon et al., 2017) with existing instruments. We recommend that future spectrographs on large telescopes (1) plan to incorporate gratings that will provide a spectral resolution of at least $R = 6000$ at the wavelength of the Ca triplet absorption lines ($\sim$ 8500 Å) and/or the Mg b triplet ($\sim$ 5200 Å), and (2) are designed to maximize stability. Milky Way satellite galaxies typically have half-light radii of $\sim 10'$, so the larger the field of view and multiplexing that can be achieved, the more efficiently the observations can be obtained.

A key ELT goal should be to measure the radial velocities and proper motions of 300 stars per galaxy in several Milky Way satellites, with a typical accuracy per star of 3 km s^{-1} (Fig. 1). These measurements will directly determine the velocity anisotropy of the stellar orbits within each dwarf, enabling tight constraints to be placed on the inner density profiles of their dark matter halos. Observations of multiple dwarf galaxies will determine the range of halo profiles that exist and avoid the possibility of being misled by the unique history of any individual galaxy.

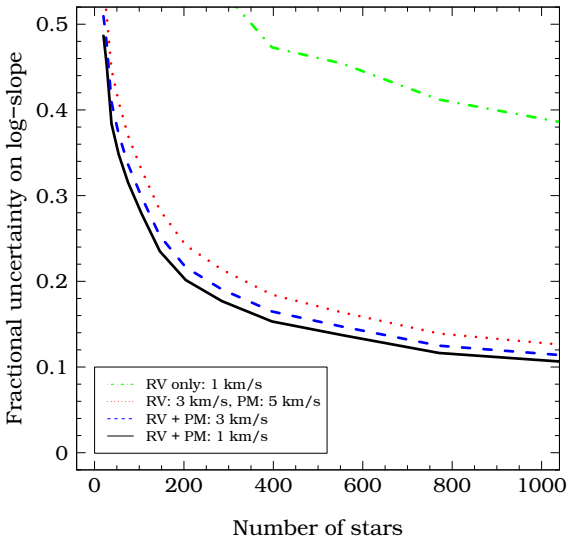

Figure 1: Simulated recovery of the dark matter density profile of a dwarf spheroidal via stellar kinematic data (based on the results of Strigari et al. 2007). Including 3D stellar velocities (red/blue/black curves) dramatically reduces the uncertainty on the central slope of the density profile relative to a data set consisting only of radial velocities (green curve). For a sample of 300 stars with proper motion and radial velocity uncertainties of 3 km s^{-1}, the expected measurement uncertainty on the slope is 0.2, enabling a 5σ detection of a central density cusp.

The ideal targets for this experiment should satisfy the following criteria: (1) Low stellar mass ($< 10^6$ M$_\odot$), to minimize stellar feedback effects on the galaxy's mass distribution; (2) High stellar surface density, to minimize the number of pointings needed to reach a sample of 300 proper motion measurements; (3) Large velocity dispersion, to increase the expected proper motion signal; (4) Small distance, to increase the expected proper motion signal and maximize the brightness of each star; and (5) An orbit that does not approach the Milky Way too closely, to minimize the

impact of Galactic tides on the structure of the dwarf. Clear choices include Draco and Ursa Minor in the north, and Sculptor and Carina in the south. Simple ELT exposure time estimates indicate that the required tangential velocity accuracy of 3 km s^{-1} can be obtained with ~ 16 hr integrations per pointing and a time baseline of 5 years. Imaging of 5 pointings per galaxy would provide a sample size of 300 stars in each target. The dark matter density profile of one dwarf could therefore be measured with a total investment of ~ 160 hrs.

ELTs offer several key advantages over space-based observing platforms for this project. In particular, the angular resolution of ELTs is an order of magnitude better than that of HST at the same wavelength. The demonstrated astrometric performance of HST relative to its diffraction limit is comparable to that expected for ELT imagers, providing a factor of ~ 5 advantage for ELTs. Furthermore, the enormous increase in collecting area means that ELTs can provide significantly larger stellar samples in a dwarf galaxy by detecting fainter stars at high S/N. On the other hand, the HST field of view is a factor of ~ 35 larger than planned first-generation ELT instruments, providing a significant increase in efficiency in the case where a large area must be observed. For the dwarf spheroidal observations described above, the proper motion measurement that can be obtained in 5 years with an ELT would require a time baseline of ~ 25 years with HST.

Strong gravitational lensing: Constraining dark matter using strong lens systems requires high-sensitivity and high-angular resolution imaging and spectroscopy. For the gravitational imaging technique, comparisons of HST vs. Keck AO imaging data have confirmed that sensitivity scales with image resolution. The current AO system on Keck produces typical angular resolutions of $60 - 90$ mas and a Strehl ratio of $\sim 10 - 30\%$ for off-axis targets. With a bigger mirror, a better AO system, and a larger population of potential tip-tilt stars, ELTs will perform significantly better. The AO systems on next-generation telescopes are designed to reach Strehl ratios as high as 90% in the K band. Furthermore, they will include built-in PSF reconstruction software that provides a model of the PSF for data analysis. The combination of improvements in resolution, sensitivity, and PSF quality and knowledge will make the ELTs much more capable than current systems. Specifically, only the brightest handful of lenses in the sky can currently be targeted with $8 - 10$ m class telescopes. The US ELT program, on the other hand, will provide virtually full sky access, allowing us to target large samples of rare quadruply-imaged objects, selecting the ones with the best (i.e., the ones containing the most structure) extended images for the gravitational imaging technique. Moreover, Fisher analyses of simulated data have shown that lens modeling of spectroscopically resolved images can mitigate the source-subhalo degeneracies, drastically increasing the sensitivity of the observations to low-mass subhalos (Hezaveh et al., 2013).

For the flux-ratio anomaly technique, a very promising route forward is AO-assisted IFU spectroscopy. Integral field spectroscopy allows the measurement of flux ratios from the narrow-line region of the AGN, which should be immune to microlensing (see Nierenberg et al., 2014; Nierenberg et al., 2017). Unfortunately the technique is currently restricted to only a handful of quads, given the limitations of tip-tilt stars and the need to have narrow lines fall in transparent windows of the Earth's atmosphere. As in the case of gravitational imaging, a two-hemisphere US ELT system will enable the application of the technique to the samples required to reach definitive conclusions on the nature of dark matter by virtue of their sensitivity (exploiting the D^4 advantage of point sources in diffraction-limited mode), resolution (for astrometry of images), and full-sky access.

In order to measure the dark matter halo mass function in the range $10^7 - 10^{10}$ $M_\odot$, forward modeling simulations indicate that samples of ~ 50 extended arcs and $\gtrsim 50$ quadruply-imaged quasars would be needed. The former provide sufficient statistics of the rarer 10^{9-10} $M_\odot$ substruc-

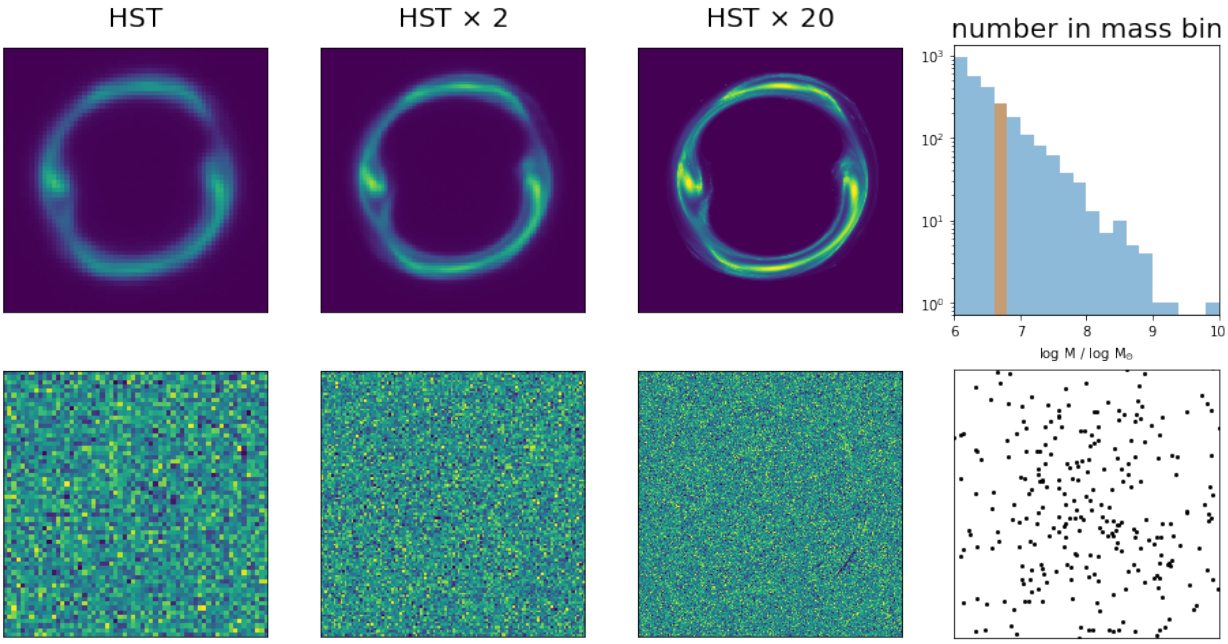

Figure 2: The effect of lensing substructure on a resolved arc for three different imaging resolutions. The baseline (left panel) illustrates an HST image with FWHM 0.1″, followed by a ground based AO observation of FWHM 0.05″ (second panel) and an ELT-like observation with FWHM 0.005″ (third panel). Top row: simulated images. Bottom row: residuals per pixel (in S/N) between a simulation with the substructure signal and without the presence of lensing substructure. For this particular simulation, we only included substructure in the mass range $10^{6.6-6.8}$ $M_\odot$. The imprint of these low-mass structures is only detectable in the ELT simulation (third panel, bottom row).

tures, while the latter are needed for direct and statistical constraints on the mass function in the range 10^{7-9} $M_\odot$. For the gravitational imaging technique, the brighter the source galaxy, the more clumpy its structure, and the better the separation between the lens galaxy and the background lensed object, the better the substructure constraints will be. The sample of lenses should contain low and high redshift lenses (and sources) to statistically break the degeneracy between LOS structure and subhalos bound to the main deflector and characterize possible evolutionary trends. Gravitational imaging will be able to provide additional constraints on the inner density slope of the massive subhalos ($\sim$ 10^{10} $M_\odot$). Observations of each lens system are expected to require integration times of a few hours on an ELT.

3 Summary

We suggest that two complementary ELT experiments could provide fundamental tests of whether dark matter is cold and non-interacting by means of (1) the 3D motions of stars in nearby dwarf galaxies and (2) gravitational lensing of distant galaxies and quasars. The dwarf galaxy component of this program would employ diffraction-limited imaging (combined with deep spectroscopy) to measure the 3D velocities of ~ 300 stars in each of two Milky Way satellite galaxies. The lensing component of the program would focus on diffraction-limited, high S/N IFU spectroscopy of 50 multiply-imaged quasars and 50 resolved arcs. Investment of $\sim$ 600 hrs of ELT time in these projects would result in unparalleled constraints on the dark matter density profiles of undisturbed halos and the subhalo mass function on scales well below those probed by luminous structures.

References

Adams, E. A. K., Oosterloo, T. A., Cannon, J. M., Giovanelli, R., & Haynes, M. P. 2016, A&A, 596, A117

Adams, J. J., Simon, J. D., Fabricius, M. H., et al. 2014, ApJ, 789, 63

Amorisco, N. C., & Evans, N. W. 2012, MNRAS, 419, 184

Battaglia, G., Helmi, A., Tolstoy, E., et al. 2008, ApJ, 681, L13

Birrer, S., Amara, A., & Refregier, A. 2017, JCAP, 5, 037

Bonaca, A., Hogg, D. W., Price-Whelan, A. M., & Conroy, C. 2018, submitted to ApJ, arXiv:1811.03631

Breddels, M. A., Helmi, A., van den Bosch, R. C. E., van de Ven, G., & Battaglia, G. 2013, MNRAS, 433, 3173

Bullock, J. S., & Boylan-Kolchin, M. 2017, ARA&A, 55, 343

Carlberg, R. G. 2012, ApJ, 748, 20

Chakrabarti, S., Bigiel, F., Chang, P., & Blitz, L. 2011, ApJ, 743, 35

Chakrabarti, S., & Blitz, L. 2009, MNRAS, 399, L118

Dalal, N., & Kochanek, C. S. 2002, ApJ, 572, 25

Despali, G., Vegetti, S., White, S. D. M., Giocoli, C., & van den Bosch, F. C. 2018, MNRAS, 475, 5424

Di Cintio, A., Brook, C. B., Macciò, A. V., et al. 2014, MNRAS, 437, 415

Gilman, D., Agnello, A., Treu, T., Keeton, C. R., & Nierenberg, A. M. 2017, MNRAS, 467, 3970

Governato, F., Zolotov, A., Pontzen, A., et al. 2012, MNRAS, 422, 1231

Hezaveh, Y., Dalal, N., Holder, G., et al. 2013, ApJ, 767, 9

Hezaveh, Y. D., et al. 2016, Astrophys. J., 823, 37

Hsueh, J.-W., Despali, G., Vegetti, S., et al. 2018, MNRAS, 475, 2438

Hsueh, J. W., Fassnacht, C. D., Vegetti, S., et al. 2016, MNRAS, 463, L51

Hsueh, J. W., Oldham, L., Spingola, C., et al. 2017, MNRAS, 469, 3713

Kaplinghat, M., Tulin, S., & Yu, H.-B. 2016, Phys. Rev. Lett., 116, 041302

Kirby, E. N., Simon, J. D., & Cohen, J. G. 2015, ApJ, 810, 56

Klypin, A., Kravtsov, A. V., Valenzuela, O., & Prada, F. 1999, ApJ, 522, 82

Koopmans, L. V. E. 2005, MNRAS, 363, 1136

Kravtsov, A. 2010, Advances in Astronomy, 2010, 8

Li, R., Frenk, C. S., Cole, S., Wang, Q., & Gao, L. 2017, MNRAS, 468, 1426

Mao, S., & Schneider, P. 1998, MNRAS, 295, 587

Metcalf, R. B., & Madau, P. 2001, ApJ, 563, 9

Moore, B., Ghigna, S., Governato, F., et al. 1999, ApJ, 524, L19

Navarro, J. F., Frenk, C. S., & White, S. D. M. 1996, ApJ, 462, 563

Navarro, J. F., Hayashi, E., Power, C., et al. 2004, MNRAS, 349, 1039

Newman, A. B., Treu, T., Ellis, R. S., & Sand, D. J. 2013, ApJ, 765, 25

Nierenberg, A. M., Treu, T., Wright, S. A., Fassnacht, C. D., & Auger, M. W. 2014, MNRAS, 442, 2434

Nierenberg, A. M., Treu, T., Brammer, G., et al. 2017, MNRAS, 471, 2224

Oh, S.-H., Brook, C., Governato, F., et al. 2011, AJ, 142, 24

Oh, S.-H., Hunter, D. A., Brinks, E., et al. 2015, AJ, 149, 180

Ritondale, E., Vegetti, S., Despali, G., et al. 2019, MNRAS, in press, arXiv:1811.03627

Simon, J. D., & Blitz, L. 2002, ApJ, 574, 726

Simon, J. D., Li, T. S., Drlica-Wagner, A., et al. 2017, ApJ, 838, 11

Spergel, D. N., & Steinhardt, P. J. 2000, Phys. Rev. Lett., 84, 3760

Springel, V., Wang, J., Vogelsberger, M., et al. 2008, MNRAS, 391, 1685

Strigari, L. E., Bullock, J. S., Kaplinghat, M., et al. 2007, ApJ, 669, 676

Strigari, L. E., Frenk, C. S., & White, S. D. M. 2017, ApJ, 838, 123

Vegetti, S., Koopmans, L. V. E., Auger, M. W., Treu, T., & Bolton, A. S. 2014, MNRAS, 442, 2017

Vegetti, S., Koopmans, L. V. E., Bolton, A., Treu, T., & Gavazzi, R. 2010, MNRAS, 408, 1969

Vegetti, S., Lagattuta, D. J., McKean, J. P., et al. 2012, Nature, 481, 341

Wright, S. A., Walth, G., Do, T., et al. 2016, in Proc. SPIE, Vol. 9909, Adaptive Optics Systems V, 990905

Xu, D., Sluse, D., Schneider, P., et al. 2016, MNRAS, 456, 739